Computers in Biology and Medicine 89 (2017) 18–23

Contents lists available at ScienceDirect

Computers in Biology and Medicine

journal homepage: www.elsevier.com/locate/compbiomed

Machine-learning-based classification of real-time tissue elastography for hepatic fibrosis in patients with chronic hepatitis B

Yang Chen [a,b], Yan Luo [b,**], Wei Huang [a], Die Hu [a], Rong-qin Zheng [c], Shu-zhen Cong [d], Fan-kun Meng [e], Hong Yang [f], Hong-jun Lin [g], Yan Sun [h], Xiu-yan Wang [i], Tao Wu [c], Jie Ren [c], Shu-Fang Pei [d], Ying Zheng [e], Yun He [f], Yu Hu [g], Na Yang [h], Hongmei Yan [a,*]

[a] Center for Information in Biomedicine, University of Electronic Science and Technology of China, Chengdu 610000, China
[b] Department of Ultrasound, West China Hospital, Sichuan University, Chengdu 610000, China
[c] Department of Ultrasound, Third Affiliated Hospital, Sun Yat-sen University, Guangzhou 510000, China
[d] Department of Ultrasound, Guangdong General Hospital, Guangzhou 510000, China
[e] Department of Ultrasound, Beijing Youan Hospital, Capital Medical University, Beijing 100000, China
[f] Department of Ultrasound, First Affiliated Hospital, Guangxi Medical University, Nanning 530000, China
[g] Department of Ultrasound, Jiangsu Province Hospital, Nanjing 210000, China
[h] Department of Ultrasound, Second Affiliated Hospital, Kunming Medical University, Kunming 650000, China
[i] Department of Ultrasound, Tongji Hospital, Tongji University, Shanghai 200000, China

ARTICLE INFO

Keywords:
Machine learning
Chronic hepatitis B
Hepatic fibrosis
Real-time tissue elastography

ABSTRACT

Hepatic fibrosis is a common middle stage of the pathological processes of chronic liver diseases. Clinical intervention during the early stages of hepatic fibrosis can slow the development of liver cirrhosis and reduce the risk of developing liver cancer. Performing a liver biopsy, the gold standard for viral liver disease management, has drawbacks such as invasiveness and a relatively high sampling error rate. Real-time tissue elastography (RTE), one of the most recently developed technologies, might be promising imaging technology because it is both noninvasive and provides accurate assessments of hepatic fibrosis. However, determining the stage of liver fibrosis from RTE images in a clinic is a challenging task. In this study, in contrast to the previous liver fibrosis index (LFI) method, which predicts the stage of diagnosis using RTE images and multiple regression analysis, we employed four classical classifiers (i.e., Support Vector Machine, Naïve Bayes, Random Forest and K-Nearest Neighbor) to build a decision-support system to improve the hepatitis B stage diagnosis performance. Eleven RTE image features were obtained from 513 subjects who underwent liver biopsies in this multicenter collaborative research. The experimental results showed that the adopted classifiers significantly outperformed the LFI method and that the Random Forest(RF) classifier provided the highest average accuracy among the four machine algorithms. This result suggests that sophisticated machine-learning methods can be powerful tools for evaluating the stage of hepatic fibrosis and show promise for clinical applications.

1. Introduction

Hepatic fibrosis is the middle stage of hepatitis of various types, of liver cirrhosis and of any late period liver-related diseases. Patients with hepatitis C or B virus who chronically suffer from fibrosis are more vulnerable to hepatocellular carcinoma. Therefore, early detection and prompt intervention are important. It has been reported that more aggravated hepatic fibrosis increases the risk of hepatocellular carcinoma [1]; however, some interferon treatments can slow this process and reduce morbidity from hepatocellular carcinoma [2], which is why the *Guide to the Prevention and Treatment for Chronic Hepatitis B* considers it essential to evaluate the stage of hepatic fibrosis both for treatment and

* Corresponding author.
** Corresponding author.
E-mail addresses: sophie-0627@163.com (Y. Chen), luoyan15957@126.com (Y. Luo), lembert1990@163.com (W. Huang), 15182510600@163.com (D. Hu), zssyzrq@163.com (R.-q. Zheng), shzhcong@163.com (S.-z. Cong), mengfankun818@126.com (F.-k. Meng), yanghonggx@163.com (H. Yang), linhongjun0909@163.com (H.-j. Lin), 1131191506@qq.com (Y. Sun), tjwangxiuyan@163.com (X.-y. Wang), wutao83@126.com (T. Wu), renjieguangzhou@126.com (J. Ren), peishufang2008@163.com (S.-F. Pei), xl2264@126.com (Y. Zheng), heyungx@gmail.com (Y. He), helenhuyu@163.com (Y. Hu), yangna627@126.com (N. Yang), hmyan@uestc.edu.cn (H. Yan).

http://dx.doi.org/10.1016/j.compbiomed.2017.07.012
Received 14 January 2017; Received in revised form 14 July 2017; Accepted 17 July 2017

for monitoring treatment effects.

However, determining the stage of liver fibrosis is still arduous. Although a liver biopsy is widely considered the gold standard for assessing liver fibrosis, the procedure's invasiveness can cause complications such as hemorrhage and pneumothorax. Moreover, limited sample numbers and sizes usually lead to suboptimal accuracy [3–5]. Another option, serological examination, has some clinical implications; however, it has been reported that its sensitivity and specificity vary greatly. Moreover, serological examination cannot satisfy the requirements for clinical treatments by itself because it is unable to accurately stage liver fibrosis [6,7]: it can distinguish between hepatic fibrosis and cirrhosis but cannot accurately determine the stage of hepatic fibrosis. In addition, this type of examination is not sufficiently specific because it can be affected by metabolism, extracellular-matrix diseases and late-stage cancers [8]. Therefore, the Asian-Pacific Association for the Study of the Liver recommends elastography instead of serological examination. Many scholars have sought other noninvasive methods to diagnose liver fibrosis, especially physical methods.

One existing noninvasive method is imaging diagnosis, which can completely evaluate the entire organ. Therefore, imaging examination has been widely adopted clinically. Imaging diagnosis can involve ultrasound, Computed Tomography (CT) or Magnetic Resonance Imaging (MRI); of these, CT and MRI are expensive. Ultrasound is the most feasible and inexpensive method. Unlike the others, it is suitable for use on patients with medical metal devices; consequently, ultrasound is widely accepted. Owing to the prevalence of ultrasound contrast and ultrasonic elastography, ultrasound can provide not only information about hepatic morphology and blood dynamics but also information about physical properties such as liver stiffness or elasticity modulus. In view of this capacity, ultrasound may emerge as one of the most important noninvasive methods for evaluating liver fibrosis.

RTE is also increasing in popularity and is considered to be among the most promising methods for staging hepatic fibrosis; however, it is unable to distinguish between intermediate degrees of liver fibrosis [9]. The calculations of both the elastic ratio and fibrosis index of RTE have shown intra-and inter-observer variability [10]. These methods have already been applied to the research of hepatitis C [11], non-alcoholic liver disease [12] and hepatitis B [13]. However, their classification accuracy reaches only approximately 70% for chronic hepatitis B patients, which cannot satisfy clinical demands.

A similar study conducted by Wu et al. [13] obtained predictions of significant fibrosis with the help of a multiple regression statistical analysis. However, multiple regression is a linearly dependent method, while the relationships between the image parameters and stages of hepatitis B are not linear.

As we know, machine-learning (ML) and pattern-recognition methods have been widely studied for early diagnosis of hepatitis diseases, such as in analyses of biochemical indices and clinical figures of hepatic fibrosis [14–25]. However, because FibroScan has been adopted for assessing the stage of liver fibrosis in recent years [26–28], studies have seldom been conducted to evaluate the performance of machine learning in real-time ultrasonic tissue elastography. This paper focuses on the analysis of data in patients with chronic hepatitis B via RTE. The data indicate the rigidity of tissue indirectly by the displacement caused by mechanical heart impulses. The RTE software was developed by Hitachi (HI VISION Ascendus; Hitachi Aloka Medical, Tokyo, Japan) and offers 11 parameters to facilitate the quantitative evaluation of liver fibrosis [29,11]. A total of 513 subjects suffering from chronic viral hepatitis and cirrhosis were studied and enrolled in a multicenter collaborative hospital study. Four classical pattern-recognition methods, which included Naïve Bayes, Random Forest (RF), K-Nearest Neighbor (KNN) and Support Vector Machine (SVM), were applied to build an aided decision-support system to estimate the stage of hepatic fibrosis.

The remainder of the paper is organized as follows. Section 2 presents a brief introduction to the four machine-learning methods used in this study. Section 3 focuses on the study methodology, in which RTE images were acquired to extract features and to perform further data preprocessing. Section 4 presents the experimental results. Finally, Section 5 draws conclusions, discusses the findings, and describes some plans for future work.

2. Machine-learning-based classification

The existing method, which is intended to determine the fibrosis stage via RTE, is to obtain the LFI as the fibrosis index [13] using a linear regression equation. However, this type of equation has limited functionality, and satisfactory results are often difficult to obtain. In this paper, we employ four classical machine learning methods to predict the stage of hepatic fibrosis based on features extracted from numerous RTE images. Our approach will improve the accuracy of staging hepatic fibrosis based on RTE, and the performances of the four classifiers will be assessed based on specific tasks. In this section, we briefly summarize the basic concepts and properties of these classifiers, which include the Naïve Bayes Classifier, Random Forest, K-Nearest Neighbor, and the Support Vector Machine.

2.1. Naïve Bayes Classifier

The Naïve Bayes classifier is a type of probabilistic classifier that is built directly on the Bayes theorem, i.e., predicting the class of a given sample by computing the maximum posterior probability based on the prior probability and the observed likelihood in the training set. Although it relies on this bold assumption, the Naïve Bayes classifier usually achieves good results in many practical application situations.

2.2. Random Forest (RF)

The Random Forest is a typical ensemble learning method that attempts to obtain a strong classifier by combining the predictions of multiple decision trees (individual decision tree can be regarded as a weak classifier). The RF classifier can usually weaken the overfitting problem that often occurs with individual decision-tree classifier. In addition, Random Forest is robust to situations in which the feature vectors contain discrete values.

2.3. K-Nearest Neighbor (KNN)

The K-Nearest Neighbor classifier is one of the exemplar-based statistical learning algorithms. Different from most learning algorithms, where building the model during the training stage involves high costs, the KNN method simply projects the original training data to the feature space during the training stage. Then, the test sample's classification is determined based on the labels of the K nearest training samples in the feature space. In addition, some distance measures are usually adopted to determine the contributions of the K neighbors.

2.4. Support vector machine (SVM)

A support vector machine aims to find the super hyperplane with the largest margin between positive and negative samples in the feature space. Thus, an SVM classifier can achieve good generalization ability during the testing phase from the test samples. In addition, some kernel functions (e.g., Gaussian Kernel, Radial Basis Function, etc.) are usually used to project the data from a low dimensional to a high dimensional feature space to improve linear separability as much as possible.

3. Methods

3.1. Acquiring RTE images

The RTE equipment used in this research was a color Doppler ultrasound diagnostic instrument, the Hitachi HI VISION Preirus (Hitachi

Aloka Medical Corporation, Tokyo Japan) and a EUP-L52 linear probe (Hitachi Aloka Medical) with a frequency range of 3–7 MHz. This instrument is equipped with real-time elastography software that can analyze tissue dispersion quantitatively, attaining 11 elastography parameters. The equipment is also equipped with a strain histogram measurement data-processing system. All the RTE examinations were conducted with this platform.

The patients in the research were enrolled in the China multi-centered real-time elastography of liver fibrosis of hepatitis B project. These subjects are the same group used in the previous study by Wu et al. [13]. Patients were placed in a supine position or in left lateral clinostatism if necessary. The probe was placed within the range of the right anterior axillary line and the midaxillary line of the fifth and eighth ribs. A two-dimensional ultrasonic examination was performed to reveal the hepatic tissue in the hepatic right anteroinferior segment, also called S5 according to Couinaud's anatomy, avoiding the cross-section of the large intrahepatic vessels and limb shadows and obtaining a vertical image to determine the direction of the heart impulse. Subsequently, the subjects underwent an ultrasonic elastography dispersed quantitative investigation with the help of the preset hepatic elastographic imaging conditions of the equipment. Leaving all settings unchanged on the equipment, a sample frame with an area of 2.5 cm × 2.5 cm was placed on an area of liver parenchyma approximately 0.5–1 cm from the liver surface. During sample collection, patients held their breath. When an elastography curve emerged with five stable waves according to the heart impulse, the image was frozen and three or five stable waves were obtained before dispersed quantitative analysis of their troughs (Figs. 1 and 2). Each time, eleven elastography parameters were expected to be obtained, and their average values were recorded. Both dynamic and static images were stored on disks.

The fibrosis stages were determined by the outcomes of liver biopsies, the procedure that is believed to be the gold standard. Advanced, US-guided percutaneous liver biopsies targeted the same position in the liver as the RTE method described above. A 1.2-mm-diameter and 160-mm-long needle was used to perform the biopsy, which was performed one week before the RTE checkup. Hepatic tissue from the biopsy was immersed in formaldehyde before being enclosed in paraffin and stained with hematoxylin-eosin. The results were produced by senior pathologists who were not informed of the ultrasonic and serum experimental results. The liver fibrosis stage was determined according to the Scheuer scoring system, while hepatic tissue pathology [30,31], was analyzed according to the Prevention and Treatment Scheme on Virus Hepatitis, revised in 2001. Chronic hepatic fibrosis is divided into stages labeled S0—S4: (1) stage S0 indicates non-fibrosis; (2) stage S1 refers to slight fibrosis in the portal area and its vicinity as well as to limited pre-sinusoid fibrosis; (3) stage S2 represents a medium level at which fibrous septa have formed but most of the lobular architecture remains; (4) stage S3 indicates a serious progression in which large amounts of fibrous septa can be observed in the liver, which damage the lobules by separating them into smaller parts, but no cirrhosis is observed; and (5) stage S4 indicates hepatic cirrhosis.

3.2. Feature extraction based on RTE images

We extracted 11 image features to quantify the variable patterns of the RTE images. Each elastography parameter was directly obtained through the real-time elastography software installed in the RTE equipment (Hitachi HI VISION Preirus). The ranges of the 11 parameters of hepatic fibrosis in real-time elastography are listed in Table 1.

3.3. Data preprocessing

For standardization, the 13 different diagnostic parameters—the 11 RTE features, age and sex—underwent conversion according to the schemes shown in Fig. 1 [32].

(1) To function equivalently, these values were all converted to a standard range, [0,1]. For instance, a patient's age usually ranges from 0 to 100. If a patient is 55, his or her standardized value should be 55/100 (0.55), which follows the formula below:

$$\bar{x}_i = \frac{x_i - x_{\min}}{x_{\max} - x_{\min}}, \tag{1}$$

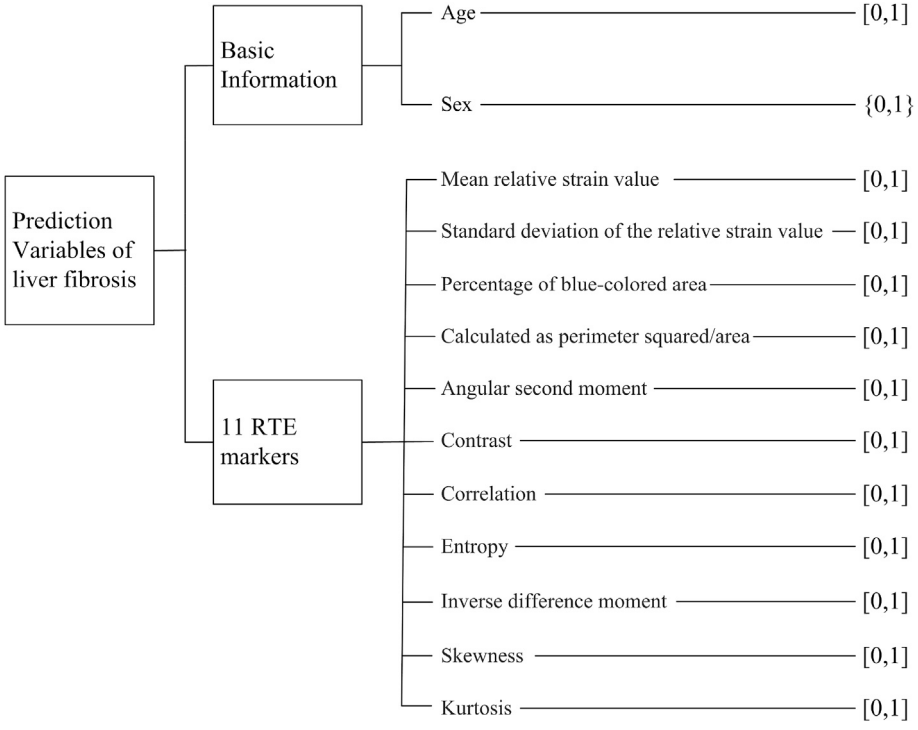

Fig. 1. List of 13 variables relevant to liver fibrosis classification and their encoding schemes.

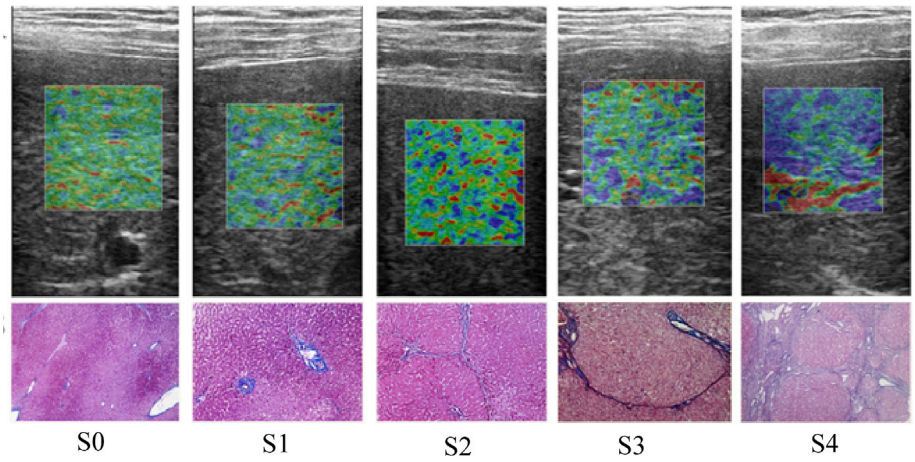

Fig. 2. Typical RTE images (top) and corresponding pathological images (bottom) for each fibrosis stage.

Table 1
Parameter ranges of hepatic fibrosis in real-time elastography.

	Attributes	Value ranges of attributes
1	mean relative strain value (MEAN)	54.49–141.24
2	standard deviation of the relative strain value (SD)	29.50–75.25
3	percentage of low-strain area (percentage of blue-color area: %AREA)	0.76–62.52
4	complexity of low-strain area (perimeter squared/area: COMP)	9.23–60.44
5	angular second moment (ASM)	0.00–0.04
6	Contrast(CONT)	63.98–353.30
7	Correlation(CORR)	0.93–0.98
8	entropy (ENT)	3.28–4.00
9	inverse difference moment (IDM)	0.09–0.28
10	skewness (SKEW)	0.18–1.23
11	kurtosis (KURT)	1.98–4.08

where x_i indicates the value of an input variable, x_{min} is the minimum of the data range, and x_{max} is the maximum of the data range.

(2) Variables with only two attributes were encoded as binary values (0, 1). For sex, 1 denoted female and 0 denoted male.

3.4. Executing the prediction

Based on the RTE images, each sample could be represented by the 13-dimensional normalized variable mentioned above. When a sample representation was input into a trained classifier, the classifier could predict the fibrosis stage of the sample. In this paper, given the large number of samples collected, it was feasible to both train the classifier and test its function. In addition, to comprehensively evaluate the performance of each classifier, accuracy, sensitivity and specificity criteria were adopted. The accuracy rate identifies the proportion of correctly classified samples among all samples, sensitivity identifies the proportion of correctly classified positive samples, and specificity identifies correctly classified negative samples [19,23].

4. Results

4.1. Data collection

The study protocol was approved by the independent ethics committees of the involved institutions, and the purpose of this research was explained to the patients. Written informed consent was obtained in advance. This prospective, multicenter, cross-sectional study was conducted at the following eight hospitals in China: Third Affiliated Hospital (Sun Yat-sen University), Guangdong General Hospital, Beijing Youan Hospital (Capital Medical University), First Affiliated Hospital (Guangxi Medical University), West China Hospital (Sichuan University), Jiangsu Province Hospital, Second Affiliated Hospital (Kunming Medical University) and Tongji Hospital (Tongji University).

The participants were selected according to the following three requirements: (1) they were being examined for pathological liver tissue; 2) they had a previous history of hepatitis B or a history of being HBsAg-positive for more than 6 months, and their HBsAg and/or HBV DNA was still positive (including both HBeAg-positive and HBeAg-negative); and 3) they underwent an ultrasonic examination. Candidates suffering from any other type of hepatitis other than hepatitis B, metabolic diseases, fatty liver or drug- or alcohol-induced liver injury were excluded [33].

As a result, 836 consecutive patients with chronic hepatitis B (CHB) or cirrhosis were selected to undergo RTE and a percutaneous US-guided liver biopsy between June 2010 and July 2013.

Samples were discarded when any of the following situations occurred: (1) the RTE images exhibited horizontal slippage caused by cardiac movement, (2) insufficient RTE images were obtained from the subject, (3) the images included artifacts or revealed low US penetration, or (4) the candidate had incomplete pathologic results. In total, 89 patients were excluded due to poor-quality images and 234 were excluded because of inadequate clinical materials, resulting in a total of 513 samples used for analysis. The subjects included 341 male and 172 female patients aged 18–72 years. The patients' clinical characteristics and laboratory information are listed in Table 2.

Fig. 2 shows typical RTE images and pathological images for each fibrosis stage. Fig. 2 shows that as the stage of hepatic fibrosis increased, the real-time elastography varied from an even green distribution to ones with randomly distributed blue parts that increased during the progression to hepatic fibrosis.

The numerical distribution of the hepatic fibrosis stages of the 513

Table 2
Clinical characteristics and laboratory information of the study patients.

Characteristics and laboratory information	Mean ± SD
Age, years	38.102 ± 13.01
Body mass index	21.787 ± 2.820
AST, IU/l	60.502 ± 77.747
ALT, IU/l	83.908 ± 123.976
Albumin, g/dl	42.152 ± 4.535
Total bilirubin, mg/dl	25.680 ± 45.396
GGT, IU/l	137.757 ± 249.299
ALP, IU/l	123.201 ± 144.937
Platelet count, $\times 10^4$ /L	197.538 ± 63.414
Prothrombin time, %	103.393 ± 15.464

Table 3
The numerical distributions of the different stages of hepatic fibrosis.

	S0	S1	S2	S3	S4
Number	119	164	88	72	70
Age	34.00 ± 11.00	37.07 ± 11.06	38.17 ± 10.91	44.18 ± 11.22	48.74 ± 9.98
Male	74	113	57	49	48
Female	45	51	31	23	22

cases, which were confirmed by liver histology assessment, is shown in Table 3. The pathological results showed that there were 119 cases in stage 0, 164 cases in stage 1, 88 cases in stage 2, 72 cases in stage 3, and 70 cases in stage 4. The average age at each stage and the corresponding numbers of male and female patients are also listed in Table 3.

4.2. Prediction of the stage of liver fibrosis

The patients' ages and sexes and the 11 RTE markers were combined to produce the input features for the classifiers. The samples were divided into two independent and identical sets: a training set (learning) and a testing set (classification). Four-fold cross-validation was adopted to evaluate the classifiers' performances [34]. Classification accuracy, sensitivity, and specificity were calculated for each classifier. The pathological grading of the cases was adopted as the gold standard in this study. The disparities between each level were subtle. The rigidity values of the liver obtained via RTE obeyed a normal distribution; moreover, the values of different levels sometimes overlapped, making it difficult to separate them completely. Thus, a two-class classification was applied for hepatic fibrosis, that is, S0/S1–4, S0–1/S2–4, S0–2/S3–4, and S0–3/S4.

The Naïve Bayes, RF, KNN and SVM classifiers were trained to predict an individual's liver fibrosis degree. When distinguishing between S0 and S1–4, the accuracy, sensitivity and specificity of each of the four machine-learning algorithms are shown in Table 4. As shown in Table 4, all four classifiers achieved comparable performances in terms of accuracy; however, they had different performances in terms of sensitivity and specificity. SVM showed the highest sensitivity and the lowest specificity, while the Naïve Bayes model showed the lowest sensitivity and the highest specificity when a liver with hepatitis B virus infection and no fibrosis was analyzed. The mismatch between sensitivity and specificity in the models was caused primarily by the imbalanced numbers of samples between the two classes; here, the number of S0 samples was 119, while the number of S1–4 samples was 394.

The European Association for the Study of the Liver and the Asian-Pacific Association for the Study of the Liver suggest that patients in stages S0–1 and S2–4, which imply slight and medium-level fibrosis, respectively, should be subjected to both etiological treatment and anti-fibrosis treatment. The accuracy, sensitivity and specificity in distinguishing these stages for each of the four machine-learning algorithms are shown in Table 5. The results showed that all four of the classifiers achieved comparable performances in terms of accuracy, sensitivity and specificity in distinguishing these two classes.

Patients in stages S0–2 are considered to have medium-level fibrosis while those in S3–4 are considered to have high-level fibrosis. Patients of the latter type are approaching liver cirrhosis and may suffer clinical manifestations. Abnormal indicators can be found in the laboratory experiments. When distinguishing between S0–2 and S3–4, the accuracy, sensitivity and specificity of each of the four machine-learning algorithms are shown in Table 6. The RF classifier obtained the highest accuracy and specificity when we determined whether the liver showed serious hepatitis B virus infection and whether it required antiviral therapy in the clinic.

Patients in Stage 4 have already suffered liver cirrhosis, and careful observation of the related complications is needed. When distinguishing between S0–3 and S4, the accuracy, sensitivity, and specificity of each of the four machine-learning algorithms are shown in Table 7. From Table 7, all four classifiers achieved good accuracy; however, their sensitivity scores were fairly low because of the small proportion of subjects in stage four.

Table 4
Accuracy, sensitivity, and specificity of stages S0/S1–4.

	Accuracy	Sensitivity	Specificity
LFI	0.7934	0.7868	0.8151
Naïve Bayes	0.8044	0.7967	**0.8250**
RF	**0.8287**	0.8941	0.6499
KNN	0.8206	0.8926	0.6116
SVM	0.8147	**0.9297**	0.4625

Bold indicate the best performance of sensitivity, accuracy and specificity among the five approaches.

Based on the above results, the diagnostic efficiencies were respectable for all the classifiers. The RF classifier yielded the best average accuracy among the four machine-learning algorithms.

5. Discussion and conclusions

When applying machine learning to hepatic fibrosis, previous research has focused primarily on the prediction of survival vs. mortality groups [14,17–21,23–25]; few investigations have been conducted on the four stages of liver fibrosis [15,26–28]. Moreover, most of these have focused only on hepatitis C [15,16,28]. To our knowledge, no prior studies have applied machine-learning techniques to assess the stage of liver fibrosis in patients suffering from hepatitis B using real-time ultrasonic tissue elastography data. In this paper, we used four ML algorithms to classify liver fibrosis into four stages (S0/S1–4, S0–1/S2–4, S0–2/S3–4, and S0–3/S4) based on RTE ultrasound data. A previous study conducted by Wu et al. [13] to predict significant fibrosis used traditional statistical analysis to stage liver fibrosis in patients suffering from hepatitis C. Together with multiple regression equations, the LFI, which is a diagnostic index used to categorize liver rigidity, was established. Although the subjects in this joint study were all hepatitis B patients, the LFI diagnostic index was applied as well as BLFI, which focuses on determining the liver rigidity of hepatitis B patients, which can also be obtained via multiple regression equations. The previous study by Wu et al. [13] compared the efficacies of these two indices. The authors

Table 5
Accuracy, sensitivity, and specificity of stages S0–1/S2–4.

	Accuracy	Sensitivity	Specificity
LFI	0.7934	0.7348	0.8410
Naïve Bayes	0.8118	0.7438	0.8614
RF	**0.8118**	**0.7471**	**0.8621**
KNN	0.8118	0.7449	0.8617
SVM	0.7934	0.7222	0.8443

Table 6
Accuracy, sensitivity, and specificity of stages S0–2/S3–4.

	Accuracy	Sensitivity	Specificity
LFI	0.8246	0.7746	0.8437
Naïve Bayes	0.8522	**0.7866**	0.8738
RF	**0.8809**	0.6533	**0.9600**
KNN	0.8581	0.6419	0.9271
SVM	0.8471	0.5162	0.9579

Table 7
Accuracy, sensitivity, and specificity of stages S0–3/S4.

	Accuracy	Sensitivity	Specificity
LFI	0.8460	**0.7286**	0.8646
Naïve Bayes	0.8610	0.6866	0.8854
RF	**0.9125**	0.5126	0.9706
KNN	0.9044	0.4252	0.9755
SVM	0.9000	0.1718	**0.9917**

evaluated only the predictive performance for two groups (S0—S1 vs. S2—S4 and S0—S3 vs. S4). The results showed that the accuracies of BLFI and LFI for predicting significant fibrosis (S0—S1 vs. S2—S4) were 77.2% and 76.9%, respectively. For cirrhosis (S0—S3 vs. S4), the accuracies of BLFI and LFI were 77.7% and 79.3%, respectively. The sensitivities of BLFI and LFI for predicting significant fibrosis (S0—S1 vs. S2—S4) were 77.0% and 77.0%, respectively. For cirrhosis (S0—S3 vs. S4), the sensitivities of BLFI and LFI were 80.0% and 74.3%, respectively. The specificities of BLFI and LFI for predicting significant fibrosis (S0—S1 vs. S2—S4) were 77.3% and 76.8%, respectively. For cirrhosis (S0—S3 vs. S4), the specificities of BLFI and LFI were 77.4% and 79.8%, respectively. We compared our results (Tables 4–7) with the BLFI and LFI results from Wu et al. [13] listed above and concluded that ML achieved much higher accuracy than did the traditional statistics. However, the sensitivities and specificities of the classifiers are affected by the sample distributions. Our group's imbalanced data caused high variability in sensitivity and specificity. A solution for this issue is to obtain many more medical records to optimize the performance and stability of the systems.

In conclusion, this study applied four classical pattern-recognition methods, Naïve Bayes, RF, KNN and SVM, to build a decision-support system to estimate the stage of hepatic fibrosis based on real-time ultrasonic tissue elastography. The results reported here indicate that machine learning could be a superior method for staging hepatitis fibrosis compared to statistical methods. In addition, we believe that the proposed models could be helpful tools to assist specialists in determining the stage of hepatic fibrosis. The algorithm can be adapted for ultrasound diagnostic instruments such as the Hitachi-HI VISION Preirus (HITACHI Medical Corporation, Tokyo Japan), and the pathological classification can be estimated to provide doctors with faster and more reliable diagnostic approaches for these diseases.

However, our research is still limited in some ways. Although these models can reliably distinguish between two categories, because there is some overlap among the different stages: these models do not distinguish well among all five fibrosis stages (S0,S1,S2, S3, and S4). Furthermore, a liver biopsy is still considered the gold standard for assessing hepatic fibrosis in this research area, while intra-observer and inter-observer variability can possibly cause disparities between RTE indices and biopsies. In future research, we hope to obtain adequate data to provide a more sophisticated test set to demonstrate the generalization abilities of the models discussed in this paper.

Acknowledgments

The authors thank Zhang Qi for the data collection work, which was a valuable contribution to this study. This study was supported by the 973 Project (2013CB329401), the Natural Science Foundation of China (61573080, 91420105) and the Science and Technology Project of Sichuan Province (2015SZ0141).

References

[1] H. Yoshida, Y. Shiratori, M. Moriyama, Y. Arakawa, T. Ide, M. Sata, et al., Interferon therapy reduces the risk for hepatocellular carcinoma: national surveillance program of cirrhotic and noncirrhotic patients with chronic hepatitis C in Japan, Ann. Intern. Med. 131 (3) (1999) 174–181.

[2] Y. Shiratori, F. Imazeki, M. Moriyama, M. Yano, Y. Arakawa, O. Yokosuka, et al., Histologic improvement of fibrosis in patients with hepatitis C who have sustained response to interferon therapy, Ann. Intern. Med. 132 (7) (2000) 517–524.

[3] K.A. Gebo, H.F. Herlong, M.S. Torbenson, M.W. Jenckes, G. Chander, K.G. Ghanem, et al., Role of liver biopsy in management of chronic hepatitis C: a systematic review, Hepatology 36 (S1) (2002) S161–S172.

[4] A. Regev, M. Berho, L.J. Jeffers, C. Milikowski, E.G. Molina, N.T. Pyrsopoulos, et al., Sampling error and intraobserver variation in liver biopsy in patients with chronic HCV infection, Am. J. Gastroenterol. 97 (10) (2002) 2614–2618.

[5] P. Bedossa, D. Dargère, V. Paradis, Sampling variability of liver fibrosis in chronic hepatitis C, Hepatology 38 (6) (2003) 1449–1457.

[6] J. Jia, J. Hou, H. Ding, G. Chen, Q. Xie, Y. Wang, et al., Transient elastography compared to serum markers to predict liver fibrosis in a cohort of Chinese patients with chronic hepatitis B, J. Gastroenterol. Hepatol. 30 (4) (2015) 756–762.

[7] N.H. Afdhal, M. Curry, Technology evaluation: a critical step in the clinical utilization of novel diagnostic tests for liver fibrosis, J. Hepatol. 46 (4) (2007) 543–545.

[8] A. Suzuki, P. Angulo, J. Lymp, D. Li, S. Satomura, K. Lindor, Hyaluronic acid, an accurate serum marker for severe hepatic fibrosis in patients with non-alcoholic fatty liver disease, Liver Int. 25 (4) (2005) 779–786.

[9] D.I. Gheonea, A. Săftoiu, T. Ciurea, F. Gorunescu, S. Iordache, G.L. Popescu, et al., Real-time sono-elastography in the diagnosis of diffuse liver diseases, World J. Gastroenterol. 16 (14) (2010) 1720–1726.

[10] F. Paparo, F. Corradi, L. Cevasco, M. Revelli, A. Marziano, L. Molini, et al., Real-time elastography in the assessment of liver fibrosis: a review of qualitative and semi-quantitative methods for elastogram analysis, Ultrasound Med. Biol. 40 (9) (2014) 1923–1933.

[11] K. Fujimoto, M. Kato, M. Kudo, N. Yada, T. Shiina, K. Ueshima, Novel image analysis method using ultrasound elastography for noninvasive evaluation of hepatic fibrosis in patients with chronic hepatitis C, Oncology 84 (Suppl. 1) (2013) 3–12.

[12] A. Orlacchio, F. Bolacchi, M. Antonicoli, I. Coco, E. Costanzo, D. Tosti, et al., Liver elasticity in NASH patients evaluated with real-time elastography (RTE), Ultrasound Med. Biol. 38 (4) (2012) 537–544.

[13] T. Wu, J. Ren, S.Z. Cong, F.K. Meng, H. Yang, Y. Luo, et al., Accuracy of real-time tissue elastography for the evaluation of hepatic fibrosis in patients with chronic hepatitis B: a prospective multicenter study, Dig. Dis. 32 (6) (2014) 791–799.

[14] H.L. Chen, D.Y. Liu, B. Yang, J. Liu, G. Wang, A new hybrid method based on local fisher discriminant analysis and support vector machines for hepatitis disease diagnosis, Expert Syst. Appl. 38 (9) (2011) 11796–11803.

[15] A.M. Hashem, M.E.M. Rasmy, K.M. Wahba, O.G. Shaker, Single stage and multistage classification models for the prediction of liver fibrosis degree in patients with chronic hepatitis C infection, Comput. Meth. programs Biomed. 105 (3) (2012) 194–209.

[16] Z. Jiang, K. Yamauchi, K. Yoshioka, K. Aoki, S. Kuroyanagi, A. Iwata, et al., Support vector machine-based feature selection for classification of liver fibrosis grade in chronic hepatitis C, J. Med. Syst. 30 (5) (2006) 389–394.

[17] D. Çalişir, E. Dogantekin, A new intelligent hepatitis diagnosis system: PCA–LSSVM, Expert Syst. Appl. 38 (8) (2011) 10705–10708.

[18] M.S. Bascil, F. Temurtas, A study on hepatitis disease diagnosis using multilayer neural network with levenberg marquardt training algorithm, J. Med. Syst. 35 (3) (2011) 433–436.

[19] M.S. Bascil, H. Oztekin, A study on hepatitis disease diagnosis using probabilistic neural network, J. Med. Syst. 36 (3) (2012) 1603–1606.

[20] Y. Kaya, M. Uyar, A hybrid decision support system based on rough set and extreme learning machine for diagnosis of hepatitis disease, Appl. Soft Comput. 13 (8) (2013) 3429–3438.

[21] E. Dogantekin, A. Dogantekin, D. Avci, Automatic hepatitis diagnosis system based on linear discriminant analysis and adaptive network based on fuzzy inference system, Expert Syst. Appl. 36 (8) (2009) 11282–11286.

[22] K. Polat, S. Güneş, Hepatitis disease diagnosis using a new hybrid system based on feature selection (FS) and artificial immune recognition system with fuzzy resource allocation, Digit. Signal Process. 16 (6) (2006) 889–901.

[23] J.S. Sartakhti, M.H. Zangooei, K. Mozafari, Hepatitis disease diagnosis using a novel hybrid method based on support vector machine and simulated annealing (SVM-SA), Comput. Meth. Programs Biomed. 108 (2) (2012) 570–579.

[24] K. Polat, S. Güneş, Medical decision support system based on artificial immune recognition immune system (AIRS), fuzzy weighted pre-processing and feature selection, Expert Syst. Appl. 33 (2) (2007) 484–490.

[25] K. Polat, S. Güneş, Prediction of hepatitis disease based on principal component analysis and artificial immune recognition system, Appl. Math. Comput. 189 (2) (2007) 1282–1291.

[26] F. Gorunescu, S. Belciug, M. Gorunescu, R. Badea, Intelligent decision-making for liver fibrosis stadialization based on tandem feature selection and evolutionary-driven neural network, Expert Syst. Appl. 39 (17) (2012) 12824–12832.

[27] C. Stoean, R. Stoean, M. Lupsor, H. Stefanescu, R. Badea, Feature selection for a cooperative coevolutionary classifier in liver fibrosis diagnosis, Comput. Biol. Med. 41 (4) (2011) 238–246.

[28] R. Stoean, C. Stoean, M. Lupsor, H. Stefanescu, R. Badea, Evolutionary-driven support vector machines for determining the degree of liver fibrosis in chronic hepatitis C, Artif. Intell. Med. 51 (1) (2011) 53–65.

[29] N. Yada, M. Kudo, H. Morikawa, K. Fujimoto, M. Kato, N. Kawada, Assessment of liver fibrosis with real-time tissue elastography in chronic viral hepatitis, Oncology 84 (Suppl. 1) (2013) 13–20.

[30] P.J. Scheuer, Classification of chronic viral hepatitis: a need for reassessment, J. Hepatol. 13 (3) (1991) 372–374.

[31] P.J. Scheuer, The nomenclature of chronic hepatitis: time for a change, J. Hepatol. 22 (1) (1995) 112–114.

[32] H.M. Yan, Y.T. Jiang, J. Zhen, C.L. Peng, Q.H. Li, A multilayer perceptronbasedmedical decision support system for heart disease diagnosis, Expert Syst. Appl. 30 (2) (2006) 272–281.

[33] Liver disease, fatty liver and alcoholic liver disease study group of Chinese Medical Association, Guidelines for the diagnosis and treatment of nonalcoholic fatty liver disease and alcoholic liver disease, Chin. J. Liver Dis. 14 (3) (2006) 161.

[34] Q. Yan, H.M. Yan, F. Han, X.C. Wei, T. Zhu, SVM-based decision support system for clinic aided tracheal intubation predication with multiple features, Expert Syst. Appl. 36 (3) (2009) 6588–6592.